Hot carrier impact on photovoltage formation in solar cells

S. Ašmontas,[a] J. Gradauskas, A. Sužiedėlis, A. Šilėnas, E. Širmulis, V. Švedas, V. Vaičikauskas, and O. Žalys
Center for Physical Sciences and Technology, Vilnius LT-01108, Lithuania

(Received 6 June 2018; accepted 1 August 2018; published online 15 August 2018)

The photovoltaic effect in a GaAs *p-n* junction exposed to short laser pulses of the 1.06–3.0 μm spectral range is investigated experimentally. At a low excitation level of 1.06 μm radiation, the intraband single photon absorption of light dominates, and the photoresponse is found to be caused mainly by the hot carriers. As the laser intensity is increased, the photoresponse signal across the junction consists of two components; the hot carrier photovoltage and the classical photovoltage due to electron-hole pair generation resulting from two-photon absorption. The generation-induced photovoltage decreases with the increase in the radiation wavelength following the reduction of the two-photon absorption coefficient, while the carriers are shown to be heated by the intraband light absorption as well as by residual photon energy left over during the electron-hole pair generation. It is established that carrier heating by light reduces conversion efficiency of a solar cell not only via the thermalization process but also due to the competition of the hot carrier and the classical photovoltages which are of opposite polarities. *Published by AIP Publishing.*
https://doi.org/10.1063/1.5043155

To make the photovoltaic energy more cost-effective, one needs either to reduce the price of a solar cell or to increase its conversion efficiency by refining and developing new technologies and materials. The conversion efficiency of a single-junction semiconductor solar cell is fundamentally constrained by the Shockley-Queisser limit[1] since only the photons having energy close to the forbidden energy gap are effectively used. Photons of higher energy create electron and hole pairs, and the excess energy turns the photogenerated carriers into the hot carriers, with a nonequilibrium distribution temperature higher than the lattice.[2] A solar cell loses about 30% of incident solar energy when the hot carriers thermalize, i.e., dissipate the excess energy to the lattice.[3] Ross and Nozik proposed the idea of a hot carrier solar energy convertor in which the photogenerated hot carriers are extracted over a narrow range of energies at a rate faster than they dissipate energy to the lattice.[4] Theoretically, the conversion efficiency of such a device can reach 66%. Lately, a large number of theoretical and experimental works devoted to the development of hot carrier solar cells were carried out.[5–23] However, no hot carrier solar cell valuable for practical applications is built yet.

The hot carrier effect has been investigated in a nanoscopically thin photovoltaic *a*-Si *p-i-n* junction.[2] The increase in the open circuit voltage V_{oc} with photon energy was explained by the extraction of hot electrons generated near the collector, while in the thick junction, the decrease in V_{oc} was explained by the thermalization of hot electrons and the lattice warming. However, hot carriers not only deliver heat to the lattice but also induce hot carrier emf across a *p-n* junction.[24–26] Since the polarity of the hot carrier emf is opposite to that of the classical photovoltage U_{ph} resulting from electron-hole pair generation,[24–26] the carrier heating by light can directly reduce the efficiency of a solar cell. Moreover, warming of the lattice gives rise to the thermoelectric force across a *p-n* junction with polarity also opposite to that of U_{ph}. In addition, photons having energy lower than the forbidden energy gap are directly absorbed by the free carriers. Thus, the long-wave solar radiation also heats the carriers. Here, we show the impact of hot carriers on photoresponse signal formation across the GaAs *p-n* junction.

The samples were prepared from a *p*-type 4 μm-thick GaAs layer with a hole density of 5×10^{17} cm^{-3} grown by liquid phase epitaxy on an *n*-type GaAs substrate with an electron density of 3×10^{17} cm^{-3}. A thin p^+-layer with a hole density of 2×10^{18} cm^{-3} was additionally grown on the *p*-layer for the ohmic contact formation. The Au/Ge/Ni alloy was thermally evaporated on top and back surfaces of the structure, and metallic ohmic contacts were fabricated by the lift-off technique followed by the rapid thermal annealing. The *p-n* junction was illuminated from the epitaxial layer side through the square window etched in the p^+-layer. The response to illumination was measured in the photocurrent regime as a voltage across the 50 Ω load resistor.

For direct observation of the effect, hot carrier emf has to be separated from the classical photovoltage. In general, this could be achieved by means of employing short laser pulses with photon energy lower than the forbidden energy gap. A diode pumped solid state Nd:YAG laser NL202 (Ekspla Ltd, Lithuania) was used for direct excitation of the sample, as well as for parametric generation of longer wavelengths. The laser generated 15 ns duration pulses of the 1.064 μm radiation. The pulse repetition rate could be varied from single pulses to 1 kHz. At the laser output, irradiance could reach the maximum value of 2.7 MW/cm^2. For spectral measurements, an optical parametric oscillator (OPO) generating wavelengths from 1.43 μm to 4.8 μm was used (Fig. 1). Its active media was periodically poled lithium niobate PP-MgO:LN nonlinear $60 \times 15 \times 1$ mm^3 crystal (HC Photonics

[a]Author to whom correspondence should be addressed: steponas.asmontas@ftmc.lt

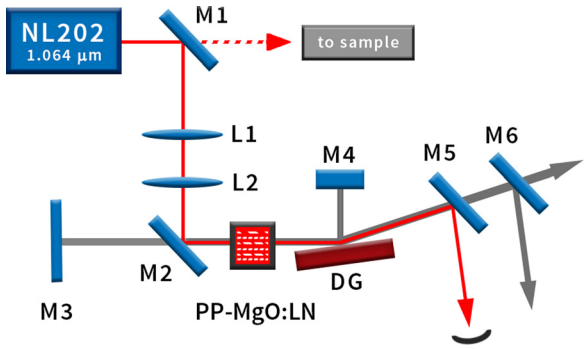

FIG. 1. Scheme of optical parametric oscillator OPO pumped by the Nd:YAG laser NL202. The 1.064 μm laser radiation is directed to the sample or, if mirror M1 is placed, is directed into the OPO; mirror M2 directs the pump radiation; L1 and L2 are lenses; mirrors M3 and M4 and the gold coated optical diffraction grating DG comprise OPO's resonant cavity; mirror M5 rejects the pump ant transmits the converted radiation; mirror M6 separates the signal and idler waves of parametric generation.

Corp., Taiwan) containing seven gratings with the period from 28.5 μm to 31.5 μm with 0.5 μm step. The crystal was placed in an electric oven (from room temperature to 200 °C) for fine thermal tuning of the wavelength. Removable mirror M1 and stationary mirror M2 directed the 1.064 μm radiation into the OPO. Lenses L1 and L2 were employed to translate the pump beam waist deep into the OPO crystal. Gold coated mirrors M3 and M4 and the gold coated optical grating (600 grooves/mm) comprised OPO's resonant cavity. Gold grating was held stable with the angle of incidence close to 90°. The grating's zero order of diffraction was used for the output of the parametric generation, while the first order of diffraction was back-reflected to the cavity path by the M4 mirror. This mirror was mounted on a rotating table with a computer controlled stepper motor. At the OPO output, mirror M5 rejected the pump and transmitted the converted radiation. The M6 dichroic mirror separated the signal and idler waves of parametric generation. The polarization of the signal and idler waves was the same as the polarization of the pump beam.

Low power 1.064 μm laser irradiation of the *p-n* junction gives rise to the photoresponse signal having the same polarity as the hot carrier emf has. The intraband single photon absorption dominates at low excitation levels and it leads to carrier heating. Since the hot carrier energy relaxation time is much shorter than the laser pulse duration, the leading front of the hot carrier photovoltage U_{hc} pulse follows that of the laser pulse (Fig. 2, trace a). The thermoelectric voltage U_T caused by the *p-n* junction heating and having the same polarity is observed together with the hot carrier photovoltage as the laser pulse ends. Since the lattice cooling time is much longer than the laser pulse duration, the trailing edge of the photoresponse signal lasts comparatively long after the laser pulse.

Two-photon absorption starts manifesting itself as the laser radiation intensity increases, and the long-lasting classical photovoltage U_{ph} of opposite polarity resulting from the electron-hole pair generation starts to be observed together with the hot carrier photovoltage (Fig. 2, trace b). The magnitude of U_{ph} initially increases with the laser intensity and follows the square law. Then, it starts saturating since the maximum value of the classical photovoltage

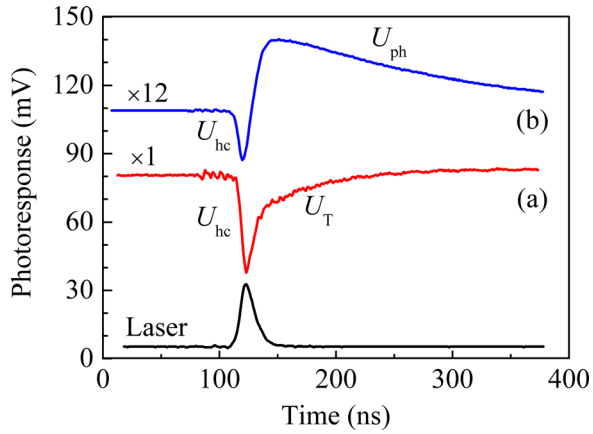

FIG. 2. Temporal shapes of the laser pulse (bottom) and photoresponse signal of the GaAs *p-n* junction under low 0.04 MW/cm^2 (a) and high 1.2 MW/cm^2 (b) intensities of 1.064 μm laser radiation. The zero point of both photoresponses is shifted in vertical for clearance, and the magnitude of U_{hc} and U_{ph} of the trace (b) should be multiplied by 12.

is limited by the potential barrier height of the *p-n* junction (see Fig. 3).

The hot carrier photovoltage linearly depends on the laser intensity at its low levels, but at higher intensities, the dependence of U_{hc} on laser intensity starts to be sublinear when the two-photon absorption becomes perceptible. Such deviation of U_{hc} from the linear law is an inherent feature of the hot carrier emf in GaAs:[27] it reaches saturation at high excitation levels as a result of the reduction of the carrier mobility and diffusion coefficient with their energy rise.[28]

The two-photon absorption coefficient β strongly depends on the radiation wavelength λ.[29,30] The measured values of classical photovoltage and hot carrier photovoltage versus wavelength within 1.06–3.0 μm range are shown in Fig. 4. U_{ph} drops down with the increasing wavelength following the reduction of the two-photon absorption coefficient value. The classical photovoltage disappears at a wavelength longer than 1.75 μm as the energy of two photons becomes lower than the GaAs forbidden energy gap.

Figure 4 shows that the dependence of U_{hc} on the wavelength differs from that of $U_{ph.}$ The hot carrier photovoltage also decreases with increasing λ. Unlike the classical

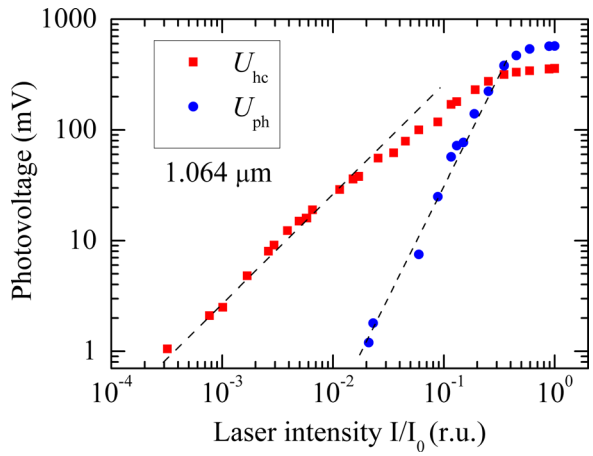

FIG. 3. Dependence of hot carrier photovoltage U_{hc} and classical photovoltage U_{ph} of the GaAs *p-n* junction on laser intensity ($\lambda = 1.064$ μm). The dashed lines are guides to the eye for linear and square dependence, respectively.

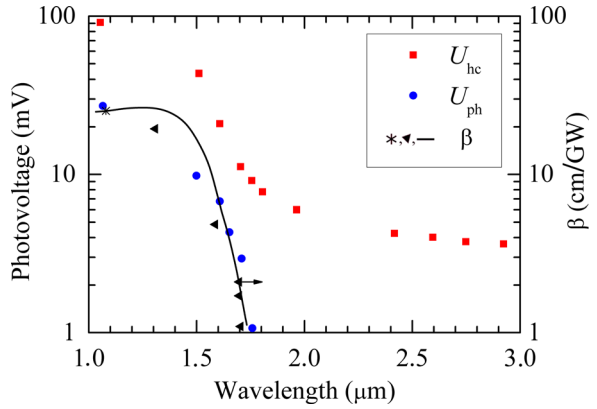

FIG. 4. Variation of hot carrier photovoltage U_{hc} and classical photovoltage U_{ph} with the wavelength at laser intensity $I = 0.22\,MW/cm^2$. Experimental data (asterisk and triangles) and theoretical solid curve of two-photon absorption coefficient β are taken from Ref. 29.

photovoltage, it does not vanish above 1.75 μm but slightly decreases as the light absorption by free electrons and holes decreases within the 1.75–3.0 μm spectral range.[28] Since the free electron absorption cross section in *n*-GaAs is larger than that of the free holes in *p*-GaAs by a factor of ten,[28,31,32] the value of U_{hc} is mainly determined by the hot electrons. Different slopes of the U_{hc} dependence on the wavelength in spectral regions $\lambda < 1.75\,\mu$m and $\lambda > 1.75\,\mu$m are worth noting. A steeper slope (stronger dependence) is seen within the observable two-photon absorption region. This finding supports the fact that the carriers are heated and thereby the hot carrier photovoltage is induced not only by the direct intraband free carrier light absorption but also by the extra energy remaining from the two-photon electron-hole pair generation.

In conclusion, we have evidenced that illumination of a *p-n* junction with short laser pulses having photon energy lower than the semiconductor forbidden energy gap permits us to observe directly simultaneous formation of the hot carrier photovoltage and the classical photovoltage. This way, carrier heating by light leads to the reduction of the conversion efficiency of a solar cell since both these photo-response voltage components have opposite polarities. Besides the usually considered thermalization of hot carriers, competition of the two photovoltages is an additional reason for the conversion efficiency of a single-junction solar cell to be always below the Shockley-Queisser limit. The presented findings can influence and considerably facilitate the design of high efficiency solar cells.

This work was supported by the Research Council of Lithuania (Grant No. 01.2.2-LMT-K-718-01-0050). The authors are grateful to Angelė Steikūnienė and Gytis Steikūnas for technical assistance in sample preparation.

[1]W. Shockley and H. Queisser, J. Appl. Phys. **32**, 510 (1961).
[2]K. Kempa, M. J. Naughton, Z. F. Ren, A. Herczynski, T. Kirkpatrick, J. Rybczynski, and Y. Gao, Appl. Phys. Lett. **95**, 233121 (2009).
[3]L. C. Hirst and N. J. Ekins-Daukes, Prog. Photovoltaics Res. Appl. **19**, 286 (2011).
[4]R. T. Ross and A. J. Nozik, J. Appl. Phys. **53**, 3813 (1982).
[5]M. Neges, K. Schwarzburg, and F. Willig, Sol. Energy Mater. Sol. Cells **90**, 2107 (2006).
[6]G. J. Conibeer, D. König, M. A. Green, and J. F. Guillemoles, Thin Solid Films **516**, 6948 (2008).
[7]G. J. Conibeer, C.-W. Jiang, D. König, S. Shrestha, T. Walsh, and M. A. Green, Thin Solid Films **516**, 6968 (2008).
[8]G. Conibeer, N. Ekins-Daukes, J.-F. Guillemoles, D. Kőnig, E.-C. Cho, C.-W. Jiang, S. Shrestha, and M. Green, Sol. Energy Mater. Sol. Cells **93**, 713 (2009).
[9]A. Le Bris and J.-F. Guillemoles, Appl. Phys. Lett. **97**, 113506 (2010).
[10]D. König, K. Casalenuovo, Y. Takeda, G. Conibeer, J. F. Guillemoles, R. Patterson, L. M. Huang, and M. A. Green, Physica E **42**, 2862 (2010).
[11]Y. Takeda and T. Motohiro, Sol. Energy Mater. Sol. Cells **95**, 2638 (2011).
[12]A. P. Kirk and M. V. Fischetti, Phys. Rev. B: Condens. Matter **86**, 165206 (2012).
[13]A. Polman and H. A. Atwater, Nat. Mater. **11**, 174 (2012).
[14]J. A. R. Dimmock, S. Day, M. Kauer, K. Smith, and J. Heffernan, Prog. Photovoltaics Res. Appl. **22**, 151 (2014).
[15]L. C. Hirst, R. J. Walters, M. F. Führer, and N. J. Ekins-Daukes, Appl. Phys. Lett. **104**, 231115 (2014).
[16]S. Saeed, E. M. L. D. de Jong, K. Dohnalova, and T. Gregorkiewicz, Nat. Commun. **5**, 4665 (2014).
[17]J. Rodière, L. Lombez, A. Le Corre, O. Durand, and J.-F. Guillemoles, Appl. Phys. Lett. **106**, 183901 (2015).
[18]G. Conibeer, S. Shrestha, S. Huang, R. Patterson, H. Xia, Y. Feng, P. Zhang, N. Gupta, M. Tayebjee, S. Smyth, Y. Liao, S. Lin, P. Wang, X. Dai, and S. Chung, Sol. Energy Mater. Sol. Cells **135**, 124 (2015).
[19]E. M. L. D. de Jong, S. Saeed, W. C. Sinke, and T. Gregorkiewicz, Sol. Energy Mater. Sol. Cells **135**, 67 (2015).
[20]Y. Zhang, C. Yam, and G. C. Schatz, J. Phys. Chem. Lett. **7**, 1852 (2016).
[21]J. A. R. Dimmock, M. Kauer, K. Smith, H. Liu, P. N. Stavrinou, and N. J. Ekins-Daukes, J. Opt. **18**, 74003 (2016).
[22]S. Chung, S. Shrestha, X. Wen, Y. Feng, N. Gupta, H. Xia, P. Yu, J. Tang, and G. Conibeer, Sol. Energy Mater. Sol. Cells **144**, 781 (2016).
[23]S. Chung, X. Wen, S. Huang, N. Gupta, G. Conibeer, S. Shrestha, T. Harada, and T. W. Kee, Sol. Energy Mater. Sol. Cells **169**, 13 (2017).
[24]M. Umeno, Y. Sugito, T. Jimbo, H. Hattori, and Y. Amemiya, Solid State Electron. **21**, 191 (1978).
[25]S. Ašmontas, J. Gradauskas, D. Seliuta, and E. Širmulis, Proc. SPIE **4423**, 18 (2001).
[26]S. Ašmontas, J. Gradauskas, A. Sužiedėlis, A. Šilėnas, E. Širmulis, V. Vaičikauskas, V. Vaičiūnas, O. Žalys, L. Fedorenko, and L. Bulat, Opt. Quantum Electron. **48**, 448 (2016).
[27]S. Ašmontas and A. Sužiedėlis, Lith. J. Phys. **33**, 45 (1993).
[28]A. Dargys and J. Kundrotas, *Handbook on Physical Properties of Ge, Si, GaAs, and InP* (Science and Encyclopedia Publishers, Vilnius, 1994).
[29]W. C. Hurlbut, Y.-S. Lee, K. L. Vodopyanov, P. S. Kuo, and M. M. Fejer, Opt. Lett. **32**, 668 (2007).
[30]S. Krishnamurthy, Z. Gang Yu, L. P. Gonzalez, and S. Guha, J. Appl. Phys. **109**, 033102 (2011).
[31]K. Osamura and Y. Murakami, Jpn. J. Appl. Phys., Part 1 **11**, 365 (1972).
[32]R. Braunstein, J. Phys. Chem. Solids **8**, 280 (1959).